Assessment of the SCAN Functional for Spin-State Energies in Spin-Crossover Systems

Jordi Cirera* and Eliseo Ruiz*
Departament de Química Inorgànica i Orgànica and Institut de Recerca de Química Teòrica i Computacional, Universitat de Barcelona,
Diagonal 645, 08028 Barcelona, Spain
email: jordi.cirera@qi.ub.es
email: eliseo.ruiz@qi.ub.es

Abstract

The Strongly-Constrained and Appropriately Normed (SCAN) functional has been tested towards the calculation of spin-state energy differences in a dataset of 20 spin-crossover (SCO) systems, ranging from d^4 to d^7. The results shown that SCAN functional is able to correctly predict the low-spin state as the ground state for all systems, and the energy window provided by the calculations falls in the approximately range of energies that will allow for SCO to occur. Moreover, because SCAN is a pure meta-GGA functional, one can use such method in periodic calculations, accounting for the effect of collective crystal vibrations and counterions in the thermochemistry of the spin-transition. Our results validate this functional as a potential method for *in silico* screening of new SCO systems at both, molecular and crystal packed levels.

1. Introduction

Spin-crossover molecules are very appealing systems either experimentally, due to their switching abilities that can be harnessed for electronic devices, or from the theoretically point of view, because of the computational challenge that accurate calculation of spin-state energy differences represents. From the experimental point of view, thousands of compounds showing such property have been characterized, mainly through magnetic measurements to determine their transition temperature $T_{1/2}$ between the low- and high-spin states. To computationally model such property, theoretical studies can adopt different strategies: (i) Despite that the magnetic properties are usually determined in solid-state powder samples, in most cases only molecular calculations are performed. (ii) The calculation of the transition temperature $T_{1/2}$ involves the inclusion of entropic contributions and, consequently the computation of the vibrational energies. This fact is particularly demanding because small errors in the vibrational energies results in relatively large errors in the entropic contributions, furthermore, in periodic boundary conditions (PBC) approaches the equivalent phonon calculations are arduous due to the lack of analytic derivatives.[1-4] (iii) Many theoretical approaches have been employed to calculate the low- high-spin state electronic energy difference. Surprisingly, highly-accurate post Hartree-Fock methods, such CASPT2 or NEVPT2 do not provide much better results than DFT approaches.[5-8] Taking into account these points, the most common theoretical approach is to study qualitatively the spin-crossover systems by performing molecular calculations.[5, 9-16] If the low-spin state is only below 10-12 kcal/mol more stable than the high spin state, such difference can be compensated with the entropic contribution and thus, the system is suitable to exhibit spin-crossover behavior. However, the quantitative calculation of the transition temperatures, as mentioned above, present many drawbacks. In order to solve some of these problems, DFT methods seem to be an appropriate approach because it is possible to perform

molecular or periodic systems calculations, analytic gradient and frequencies in molecular calculations but numerically in the PBC approaches, and relatively accurate low-high spin state energy differences. Regarding this last point, recently, we have established a benchmark set of 20 spin-crossover systems including examples of all the first-row transition metal showing such property (see Fig. 1) and moreover, they present a sharp low-high spin transition to have a well determined transition temperature. Among the high number of exchange-correlation functionals tested, only the hybrid meta-GGA TPSSh functional provides the right description of the ground state for the whole set of molecules, and relatively small low-high energy differences. The goal of this study is to apply the meta-GGA Strongly-Constrained and Appropriately Normed (SCAN) functional to verify is this non-hybrid functional can achieve similar accuracy to determine low-high electronic energy differences. This will facilitate its application in PBC approaches to handle the whole unit cell where the calculation of exact-type exchange is problematic, and it requires huge amounts of computer time. SCAN functional was developed to satisfy the all 17 exact constrains of a meta-GGA functional and consequently, is not empirical and usually, it provides results closer to the hybrid functionals than other pure meta-GGA ones. Due to its nature, the SCAN functional has attracted a lot of attention and has been tested for several applications already.[17-21]

2. Results and Discussion

A total of 20 spin-crossover systems were computed using the TPSSh and SCAN functionals. For each system, the electronic energy difference (i.e, $\Delta E = E_{HS}-E_{LS}$) was computed. In Table 1 we present the results for both functionals. The results for the

TPSSh functional have been also used to validate the computational methodology and transferability of the results (see SI).

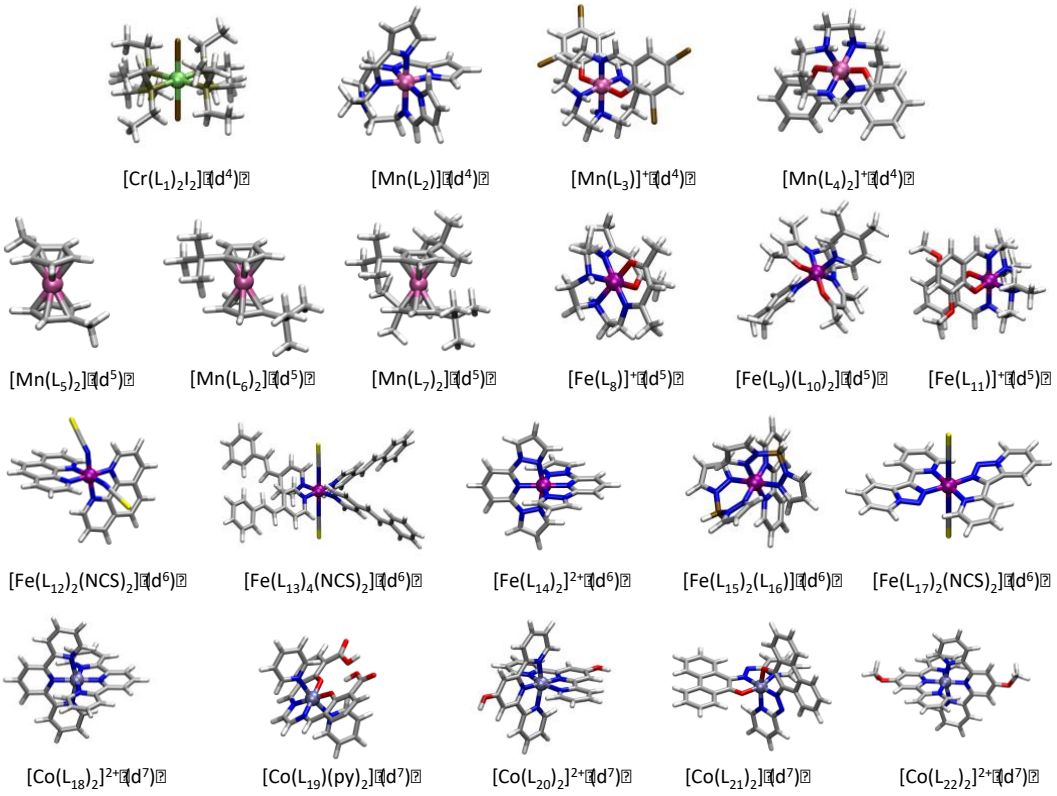

Figure 1. Data set of SCO molecules used in this work. Each row corresponds to a given electron configuration (d_4 to d_7). L_1 = 1,2-bis(Diethylphosphino)ethane-P,P', L_2 = tris(2-((Pyrrol-2-yl)methyleneamino)ethyl)amine, L_3 = 2,2'-(2,6,9,13-Tetraazatetradeca-1,13-diene-1,14-diyl)bis(4,6-dibromophenolato), L_4 = 2,2'-(2,6,9,13-tetra-azatetradeca-1,13-diene-1,14-diyl)bis(phenolato), L_5 = η_5-methylcyclopentadiene, L_6 = η_5-tert-butylcyclopentadienyl, L_7 = η_5-1,3-tert-butylcyclopentadienyl, L_8 = N_1,N_4-bis(acetylacetonato)triethylenetetramine, L_9 = ethylenebis(acetylacetoneiminato), L_{10} = 3,4-dimethylpyridyl, L_{11}= 2-(((2-(ethylamino)ethyl)imino)methyl)-6-methoxyphenolato-N,N',O, L_{12} = bis(1,10-phenanthroline-N,N'), L_{13} = 4-styrylpyridine, L_{14} = (2,6-Dipyrazol-1-yl)pyridine), L_{15} = dihydrogen bis(pyrazol-1-yl)borate, L_{16} = 2,2'-bipyridyl, L_{17} = 3-(2-pyridyl)(1,2,3)triazolo(1,5-a)pyridine, L_{18}= 2,2':6',2''-terpyridine, L_{19} = 3-formylsalicylic acid-ethylendiamine, L_{20} = 2,2':6',2''-terpyridin-4'-ol), L_{21} = 10-((pyridin-2-yl)diazenyl)phenanthren-9-olato, L_{22} = 4'-methoxy-2,2':6',2''-terpyridine.

Table 1. Electronic energy differences for all spin-crossover systems studied in this work. All energies in kcal/mol.

System	Molecule	M^{n+}	ΔE_{TPSSh}	$\Delta E_{SCAN/SG2}$	$\Delta E_{SCAN/SG3}$	ref.
S1	$[Cr(L_1)_2I_2]$	Cr^{II}	6.54	11.66	11.49	22
S2	$[Mn(L_2)]$	Mn^{III}	4.27	4.98	8.06	23
S3	$[Mn(L_3)][BF_4]$	Mn^{III}	5.53	6.24	8.54	24
S4	$[Mn(L_4)][PF_6]$	Mn^{III}	4.12	4.97	7.21	25
S5	$[Mn(L_5)_2]$	Mn^{II}	11.19	5.05	10.08	26
S6	$[Mn(L_6)_2]$	Mn^{II}	10.67	5.03	10.39	27
S7	$[Mn(L_7)_2]$	Mn^{II}	9.40	4.98	10.19	27
S8	$[Fe(L_8)][PF_6]$	Fe^{III}	9.78	5.11	11.29	28
S9	$[Fe(L_9)(L_{10})_2]$	Fe^{III}	11.45	11.41	17.61	29
S10	$[Fe(L_{11})_2][PF_6]$	Fe^{III}	10.69	8.10	14.28	30
S11	$[Fe(L_{12})_2(NCS)_2]$	Fe^{II}	6.13	8.96	13.50	31
S12	$[Fe(L_{13})_4(NCS)_2]$	Fe^{II}	8.53	9.61	16.85	32
S13	$[Fe(L_{14})_2][BF_4]_2$	Fe^{II}	9.31	15.24	20.41	33
S14	$[Fe(L_{15})_2(L_{16})]$	Fe^{II}	9.36	14.48	23.22	34
S15	$[Fe(L_{17})_2(NCS)_2]$	Fe^{II}	5.00	10.10	11.75	35
S16	$[Co(L_{18})_2]I_2$	Co^{II}	3.00	8.89	10.44	36
S17	$[Co(L_{19})(Py)_2]$	Co^{II}	2.29	4.79	8.34	37
S18	$[Co(L_{20})_2][ClO_4]_2$	Co^{II}	2.14	4.10	10.08	38
S19	$[Co(L_{21})_2]$	Co^{II}	3.78	14.02	11.80	39
S20	$[Co(L_{22})_2][BF_4]_2$	Co^{II}	6.59	8.24	10.06	40

From Table 1, one can see that the SCAN functional correctly predicts the ground state for all systems in the data set, something only attained by the TPSSh functional.[1] The effect of zero-point energy correction and dispersion correction using Grimme's D3[41] scheme implementation over the electronic energy differences have been also evaluated for the SCAN functional (Table 2). Similarly, to previously reported results, ZPE

corrected energy gaps are smaller, while the inclusion of dispersion effects increases the electronic energy differences between the two spin-states. Furthermore, it is also worth noting with the SCAN functional are much better than those provided by the pure meta GGA TPSS (see Table S2).[42]

Table 2. Electronic energy differences in kcal/mol (ΔE) for all spin-crossover systems studied in this work, as well as the zero-point energy correction (ZPE) and empirical dispersion within the Grimme's D3 scheme (D3) correction. Last column corresponds to the corrected electronic energy difference (ΔE_C = ΔE + ZPE + D3). All energies in kcal/mol

System	ΔE	ZPE	D3	ΔE_C
S1	11.66	-1.64	1.55	11.57
S2	4.98	-1.95	4.33	7.36
S3	6.24	-0.99	0.59	5.84
S4	4.97	-1.49	0.92	4.40
S5	5.05	-1.40	1.16	4.81
S6	5.03	-1.02	3.90	7.91
S7	4.98	-0.54	6.21	10.65
S8	5.11	-2.10	2.31	5.32
S9	11.41	-1.28	1.73	11.86
S10	8.10	-3.77	6.09	10.42
S11	8.96	-3.75	-1.87	3.34
S12	9.61	-1.50	-1.37	6.74
S13	15.24	-1.71	2.72	16.25
S14	14.48	-2.36	1.34	13.46
S15	10.10	-2.25	-6.07	1.78
S16	8.89	-0.59	-4.28	4.02
S17	4.79	-0.18	-3.37	1.24
S18	4.10	-0.65	6.04	9.49
S19	14.02	-1.62	1.70	14.10
S20	8.24	0.22	2.09	10.55

One of the drawbacks of the SCAN functional is the large dependence with the radial points of the grid and the requirement of highly dense grids to converge the energy values. Thus, we repeated the calculation with the Q-Chem code of the S13 system with the larger SG-3 grid (99 radial 590 angular, see Computational detail section) of 20.41 kcal/mol of electronic energy difference, this value is slightly higher than the obtained, 15.24 kcal/mol, with the SG-2 grid (75 radial 302 angular). In the Turbomole code, the suggested grid for the SCAN functional has 2475 radial points. The calculated low-high electronic energy difference using such computer code with the same basis set than in the Q-Chem code is 19.58 kcal/mol. Thus, this value is close to that found with the SG-3 grid with Q-Chem code. Recently, Mejía-Rodríguez and Trickey have proposed a deorbitalized version of the SCAN functional by replacing kinetic energy density by the Laplacian of the density.[43-44] Such new approach (SCAN-L) has a factor around three, faster than the original SCAN approach. The calculations were performed with the NWChem code using fine (70 radial 590 angular) and xfine (100 radial 1202 angular) grids and the same basis set, 18.20 and 29.49 kcal/mol, respectively. Thus, the results with such functional show slight differences in comparison with the original SCAN functional for the calculation of transition metal energetics.

Although the electronic energy differences with the SCAN functional tend to be a bit larger than the ones using TPSSh, and therefore the corresponding $T_{1/2}$ are going to be much larger than the experimental ones, the fact that the SCAN functional is a pure functional allows us to use it in the study of SCO systems in periodic conditions. This has been done for the $[Fe(bpp)_2][BF_4]_2$ system (S13 with a relatively large experimental $T_{1/2}$ of 256 K, Figure 2), for which the unit cells containing two molecules were used in the calculation of the electronic energy differences and also, as a reference system to check the influence of the grid size, The periodic calculation will allow as well to

determine the influence of the intermolecular dispersion, the intramolecular dispersion stabilize the low-spin state 2.72 kcal/mol for the S13 system per unit cell.

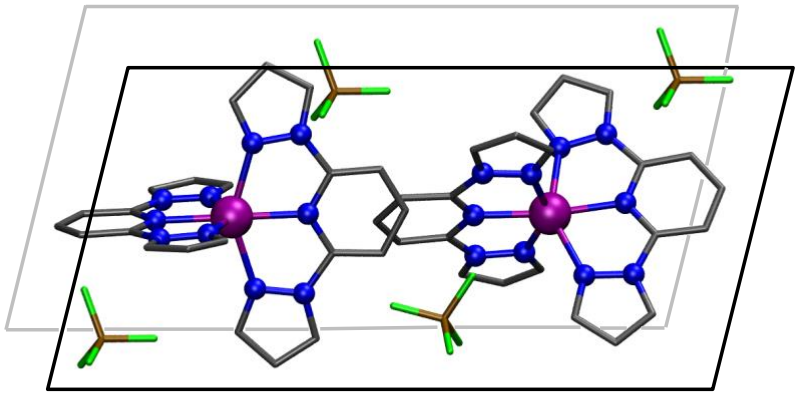

Figure 2. Unit cell for the $[Fe(bpp)_2][BF_4]_2$ system (S13) including the two crystallographic non-equivalent $[Fe(bpp)_2]^{2+}$ molecules.

A second control calculation was to use the PBC module in the Turbomole code including approximated approaches to estimate the four-center integrals using PBC but applied only to the isolated S13 molecule. The calculated value using such module for the S13 molecule is 22.34 kcal/mol. Finally, the periodic calculations including also dispersion effects through the D3 approach gives a value of 25.90 kcal/mol (24.2 kcal/mol without dispersion). This result indicates that there is an increase of the difference of the low-high energy difference. This fact is in agreement with the results found by other authors previously.[2, 4, 45-46] The analysis of the optimized low-spin cell parameters with and without dispersion indicates that the values (unit cell volumes 7802.0 and 8043.2 $Å^3$ with and without dispersion) that are closer to the available experimental low-spin structure (unit cell volume of 8697.2 $Å^3$) are those without dispersion. This fact corroborates the assumption that SCAN approach includes some important dispersion contributions.

The calculation of the thermodynamic magnitudes for the periodic model has been performed by using the post processing Phonopy code with a k-sampling using a 48x48x24 mesh in combination with the SCAN energies obtained with Turbomole code. The calculation of the phonon modes due to the lack of analytic gradients using a numerical approach results in 6N single point calculations being N the total number of atoms in the unit cell (132 atoms for the S13 system). The calculated acoustic modes that must be strictly zero in Γ point are negative and have absolute values below 0.3 cm^{-1}. The calculated entropy difference between high- and low-spin states using the optic phonons is 11.3 cal/K·mol per molecule while a value of 12.8 cal/K·mol was obtained for one isolated molecule with the SCAN functional using the Q-Chem code. Thus, the difference between both values at room temperature is only around 0.4 kcal/mol. Consequently, the use of discrete molecule to estimate the thermodynamic magnitudes could be justified taking into account the complexity of the phonon calculation in periodic systems.

Concluding Remarks

In summary, The SCAN functional has been employed to calculate the energy differences between high- and low-spin for a test case of 20 molecules. Such energy differences are very challenging from the computational point of view because most of the theoretical methods fail not only in a quantitative approach also in the prediction of the right ground state and reasonable high- and low-spin energy differences. Previously, we shown that hybrid meta-GGA TPSSh functional provided a good estimation of such energy differences with the right ground state for the whole set of calculated systems. The non-hybrid SCAN functional also gives the right ground state for the whole set of test cases being the unique pure DFT functional to provide good results for such challenging test (see Figure 3). It is worth noting the well-known large dependence of

the results with the grid size using SCAN functional. In comparison with the TPSSh functional, the calculated energy differences are slightly larger. Hence, in few cases with SCAN values are out the range to have spin transitions below room-temperature (entropy can compensate energy differences below 12 kcal/mol) but larger grids increase the number of failures

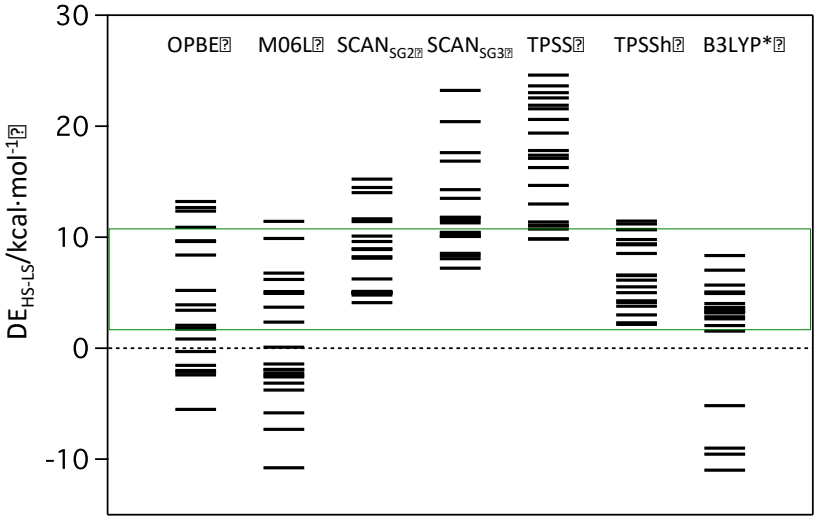

Figure 3. High- and low-spin energies for the test case with different exchange-correlation functionals. The results for the OPBE, M06L, TPSSh and B3LYP* were already published.[1] Green energy range indicates the region where the energy difference can be compensated by the entropy in a usual spin crossover system.

The lack of exact-type exchange contributions in the SCAN functional makes it more suitable for calculations with periodic boundary conditions. Thus, we have calculated the phonon spectra for the two states of one of the systems and the thermodynamic properties were extracted from the calculated frequencies. The results show that the calculation of the entropic contributions using isolated molecules provides a good estimation of such magnitude in comparison with the more complex phonon calculation of the whole unit cell.

Computational details

All Density Functional Theory calculations have been carried out with Q-Chem 5.0,[47] using a 10^{-8} convergence criterion for the density matrix elements. A fully optimized contracted triple-ζ all electron Gaussian basis set developed by Ahlrichs and co-workers with polarization functions was employed for all the elements.[48] The choice of the basis set has been done on the basis of previous results.[1] Two functionals were selected in this work, the previously used TPSSh functional,[49-50] in order to check ourselves, and the newly implemented SCAN functional.[51]. The consistency of electronic energy differences with the SCAN functional towards the integration grid has also been tested (see SI), and results seem to indicate that the standard integration grid SG-2 from Q-Chem with an unpruned 75 radial and 302 angular points (recommended for meta-GGA functionals) provides with proper results. One system was calculated with the SG-3 with 99 and 590 radial and angular points, respectively. Molecular and Periodic calculations were performed with Turbomole software, version 7.3[52] in order to compare the results with the same triple zeta basis set than the employed with Q-Chem. Furthermore, the periodic and molecular calculations were performed were done using the riper module using less-diffuse basis sets (pob-TZVP keyword) to avoid linear dependence problems and also, an auxiliary basis sets for the resolve identity approach (dhf-TZVP keyword). Dispersion effect were included using the Becke-Johnson D3 method. The grid employed in such calculations was defined through the keywords gridsize=5 and radsize=50 that it is the recommended in this code for the SCAN functional. The density of radial points also is variable for each element but is much larger than those employed with the Q-Chem code, for instance the usual reference for first-row atoms (Li-Ne) is 2475 radial points. The calculations were performed for a k-point mesh (4,4,2) including 32 k-points, these is reduction of 2.0 kcal/mol in

comparison with the (2,2,1) mesh with only 4 k-points. NWChem calculations were employed to calculate the energies using the Laplacian version of SCAN (SCAN-L) using the same basis set and the grid was defined with fine (70 radial 590 angular) and xfine (100 radial 1202 angular) grids.

Acknowledgments

The research reported here was supported by the Spanish *Ministerio de Ciencia, Innovación y Universidades* (grants PGC2018-093863-B-C21 and MDM-2017-0767). E.R. thanks Generalitat de Catalunya for an ICREA Academia award and for the SGR2017-1289 grant. The authors acknowledge computer resources, technical expertise and assistance provided by the CSUC.

References

1. Cirera, J.; Via-Nadal, M.; Ruiz, E., Benchmarking Density Functional Methods for Calculation of State Energies of First Row Spin-Crossover Molecules. *Inorg. Chem.* **2018,** *57*, 14097-14105.
2. Vela, S.; Fumanal, M.; Ribas-Arino, J.; Robert, V., Towards an accurate and computationally-efficient modelling of Fe(II)-based spin crossover materials. *PhysChemChemPhys* **2015,** *17*, 16306-16314.
3. Brehm, G.; Reiher, M.; Schneider, S., Estimation of the vibrational contribution to the entropy change associated with the low- to high-spin transition in $Fe(phen)_2(NCS)_2$ complexes: Results obtained by IR and Raman spectroscopy and DFT calculations. *J. Phys. Chem. A* **2002,** *106*, 12024-12034.
4. Fumanal, M.; Jimenez-Gravalos, F.; Ribas-Arino, J.; Vela, S., Lattice-Solvent Effects in the Spin-Crossover of an Fe(II)-Based Material. The Key Role of Intermolecular Interactions between Solvent Molecules. *Inorg. Chem.* **2017,** *56*, 4474-4483.
5. Kepp, K. P., Theoretical Study of Spin Crossover in 30 Iron Complexes. *Inorg. Chem.* **2016,** *55*, 2717-2727.
6. Phung, Q. M.; Feldt, M.; Harvey, J. N.; Pierloot, K., Toward Highly Accurate Spin State Energetics in First-Row Transition Metal Complexes: A Combined CASPT2/CC Approach. *J. Chem. Theory Comput.* **2018,** *14*, 2446-2455.
7. Radon, M., Benchmarking quantum chemistry methods for spin-state energetics of iron complexes against quantitative experimental data. *PhysChemChemPhys* **2019,** *21*, 4854-4870.
8. Song, S.; Kim, M. C.; Sim, E.; Benali, A.; Heinonen, O.; Burke, K., Benchmarks and Reliable DFT Results for Spin Gaps of Small Ligand Fe(II) Complexes. *J. Chem. Theory Comput.* **2018,** *14*, 2304-2311.

9. Cirera, J.; Paesani, F., Theoretical Prediction of Spin-Crossover Temperatures in Ligand-Driven Light-Induced Spin Change Systems. *Inorg. Chem.* **2012,** *51*, 8194-8201.
10. Cirera, J.; Ruiz, E., Theoretical modeling of two-step spin-crossover transitions in Fe-II dinuclear systems. *J. Mater. Chem. C* **2015,** *3*, 7954-7961.
11. Cirera, J.; Ruiz, E., Theoretical Modeling of the Ligand-Tuning Effect over the Transition Temperature in Four-Coordinated Fe^{II} Molecules. *Inorg. Chem.* **2016,** *55*, 1657-1663.
12. Cirera, J.; Ruiz, E., Electronic and Steric Control of the Spin-Crossover Behavior in (Cp-R)(2)Mn Manganocenes. *Inorg. Chem.* **2018,** *57*, 702-709.
13. Cirera, J.; Ruiz, E., Computational Modeling of Transition Temperatures in Spin-Crossover Systems. *Comments Inorg. Chem.* **2019,** *39*, 216-241.
14. Kepp, K. P., The ground states of iron(III) porphines: Role of entropy-enthalpy compensation, Fermi correlation, dispersion, and zero-point energies. *J. Inorg. Biochem.* **2011,** *105*, 1286-1292.
15. Kepp, K. P., Consistent descriptions of metal-ligand bonds and spin-crossover in inorganic chemistry. *Coord. Chem. Rev.* **2013,** *257*, 196-209.
16. Kepp, K. P., Heme: From quantum spin crossover to oxygen manager of life. *Coord. Chem. Rev.* **2017,** *344*, 363-374.
17. Fu, Y.; Singh, D. J., Density functional methods for the magnetism of transition metals: SCAN in relation to other functionals. *Phys. Rev. B* **2019,** *100*, 045126.
18. Mejía-Rodríguez, D.; Trickey, S. B., Analysis of over-magnetization of elemental transition metal solids from the SCAN density functional. *Phys. Rev. B* **2019,** *100*, 041113.
19. Pantazis, A. D., First-Principles Calculation of Transition Metal Hyperfine Coupling Constants with the Strongly Constrained and Appropriately Normed (SCAN) Density Functional and its Hybrid Variants. *Magnetochemistry* **2019,** *5*, 69.
20. Wang, R.; Carnevale, V.; Klein, M. L.; Borguet, E., First-Principles Calculation of Water pKa Using the Newly Developed SCAN Functional. *J. Phys. Chem. Lett.* **2019**, 54-59.
21. Yang, J. H.; Kitchaev, D. A.; Ceder, G., Rationalizing accurate structure prediction in the meta-GGA SCAN functional. *Phys. Rev. B* **2019,** *100*, 035132.
22. Halepoto, D. M.; Holt, D. G. L.; Larkworthy, L. F.; Leigh, G. J.; Povey, D. C.; Smith, G. W., Spin Crossover in Chromium(II) Complexes and the crystal and molecular structure of the high-spin form of bis 1,2-bis(diethylphophino)ethane diiodochromium(II). *J. Chem. Soc.-Chem. Commun.* **1989**, 1322-1323.
23. Sim, P. G.; Sinn, E., 1st Manganese(III) spin crossover and 1st d^4 crossover - Comment on Cytochrome-Oxidase. *J. Am. Chem. Soc.* **1981,** *103*, 241-243.
24. Pandurangan, K.; Gildea, B.; Murray, C.; Harding, C. J.; Mueller-Bunz, H.; Morgan, G. G., Lattice Effects on the Spin-Crossover Profile of a Mononuclear Manganese(III) Cation. *Chem. Eur. J.* **2012,** *18*, 2021-2029.
25. Martinho, P. N.; Gildea, B.; Harris, M. M.; Lemma, T.; Naik, A. D.; Mueller-Bunz, H.; Keyes, T. E.; Garcia, Y.; Morgan, G. G., Cooperative Spin Transition in a Mononuclear Manganese(III) Complex. *Angew. Chem.-Int. Ed.* **2012,** *51*, 12597-12601.
26. Switzer, M. E.; Wang, R.; Rettig, M. F.; Maki, A. H., Electronic ground states of manganocene and 1,1'-dimethylmanganocene. *J. Am. Chem. Soc.* **1974,** *96*, 7669-7674.

27. Walter, M. D.; Sofield, C. D.; Booth, C. H.; Andersen, R. A., Spin Equilibria in Monomeric Manganocenes: Solid-State Magnetic and EXAFS Studies. *Organometallics* **2009,** *28*, 2005-2019.
28. Dose, E. V.; Murphy, K. M. M.; Wilson, L. J., Synthesis and spin-state studies in solution of γ-substituted tris(β-diketonato) iron(III) complexes and their spin-equilibrium β-ketoimine analogues derived from triethylenetetramine. *Inorg. Chem.* **1976,** *15*, 2622-2630.
29. Maeda, Y.; Oshio, H.; Toriumi, K.; Takashima, Y., Crystal Structures, Mössbauer spectra and magnetic properties of 2 iron(III) spin-crossover complexes. *J. Chem. Soc.-Dalton Trans.* **1991**, 1227-1235.
30. Tissot, A.; Bertoni, R.; Collet, E.; Toupet, L.; Boillot, M.-L., The cooperative spin-state transition of an iron(III) compound $Fe^{III}(3\text{-MeO-SalEen})_2$ PF6: thermal- vs. ultra-fast photo-switching. *J. Mater. Chem.* **2011,** *21*, 18347-18353.
31. Gallois, B.; Real, J. A.; Hauw, C.; Zarembowitch, J., Structural changes associated with the spin transition in $[Fe(phen)_2(NCS)_2]$ - A single-crystal X-Ray Investigation. *Inorg. Chem.* **1990,** *29*, 1152-1158.
32. Roux, C.; Zarembowitch, J.; Gallois, B.; Granier, T.; Claude, R., Toward Ligand-Driven Light-Induced Spin Changing. Influence of the Configuration of 4 Styrylpyridine (stpy) on the Magnetic Properties of $[Fe^{II}(stpy)_4(NCS)_2]$ Complexes. Crystal Structures of the Spin-Crossover Species $[Fe^{II}(\textit{trans}\text{-stpy})_4(NCS)_2]$ and of the High-Spin Species $[Fe^{II}(\textit{cis}\text{-stpy})_4(NCS)_2]$ *Inorg. Chem.* **1994,** *33*, 2273-2279.
33. Carbonera, C.; Kilner, C. A.; Letard, J.-F.; Halcrow, M. A., Anion doping as a probe of cooperativity in the molecular spin-crossover compound FeL_2 BF_4 (2) (L=2,6-di{pyrazol-1-yl}pyridine). *Dalton Trans.* **2007**, 1284-1292.
34. Real, J. A.; Muñoz, M. C.; Faus, J.; Solans, X., Spin crossover in novel dihydrobis(1-pyrazoly)borate $H_2B(pz)_2$-containing iron(II) complexes. Synthesis, x-ray structure, and magnetic properties of $FeL\{H_2B(pz)_2\}_2$ (L=1,10-phenanthroline and 2,2'-bipyridine). *Inorg. Chem.* **1997,** *36*, 3008-3013.
35. Niel, V.; Gaspar, A. B.; Muñoz, M. C.; Abarca, B.; Ballesteros, R.; Real, J. A., Spin crossover behavior in the iron(II)-2-pyridyl 1,2,3 triazolo 1,5-a pyridine system: X-ray structure, calorimetric, magnetic, and photomagnetic studies. *Inorg. Chem.* **2003,** *42*, 4782-4788.
36. Figgis, B. N.; Kucharski, E. S.; White, A. H., Crystal-Structure of Bis(2,2'-6',2''-terpyridyl)cobalt(II) iodide dihydrate at 295-K and at 120-K. *Aust. J. Chem.* **1983,** *36*, 1527-1535.
37. Zarembowitch, J.; Kahn, O., Magnetic properties of some spin-crossover, high-spin, and low-spin cobalt(II) complexes with Schiff bases derived from 3-formylsalicylic acid. *Inorg. Chem.* **1984,** *23*, 589-593.
38. Gaspar, A. B.; Muñoz, M. C.; Niel, V.; Real, J. A., Co^{II}(4-terpyridone)(2) X-2: A novel cobalt(II) spin crossover system 4-terpyridone=2,6-bis(2-pyridyl)-4(1H)-pyridone. *Inorg. Chem.* **2001,** *40*, 9-10.
39. Taylor, R. A.; Lough, A. J.; Lemaire, M. T., Spin-crossover in a homoleptic cobalt(II) complex containing a redox-active NNO ligand. *J. Mater. Chem.y C* **2016,** *4*, 455-459.
40. Hayami, S.; Nakaya, M.; Ohmagari, H.; Alao, A. S.; Nakamura, M.; Ohtani, R.; Yamaguchi, R.; Kuroda-Sowa, T.; Clegg, J. K., Spin-crossover behaviors in solvated cobalt(II) compounds. *Dalton Trans.* **2015,** *44*, 9345-9348.
41. Grimme, S.; Antony, J.; Ehrlich, S.; Krieg, H., A consistent and accurate ab initio parametrization of density functional dispersion correction (DFT-D) for the 94 elements H-Pu. *The Journal of Chemical Physics* **2010,** *132*, 154104

42. Tao, J. M.; Perdew, J. P.; Staroverov, V. N.; Scuseria, G. E., Climbing the density functional ladder: Nonempirical meta-generalized gradient approximation designed for molecules and solids. *Phys. Rev. Lett.* **2003,** *91*, 146401.
43. Mejia-Rodriguez, D.; Trickey, S. B., Deorbitalization strategies for meta-generalized-gradient-approximation exchange-correlation functionals. *Phys. Rev. A* **2017,** *96*, 052512.
44. Mejia-Rodriguez, D.; Trickey, S. B., Deorbitalized meta-GGA exchange-correlation functionals in solids. *Phys. Rev. B* **2018,** *98*, 115161.
45. Bucko, T.; Hafner, J.; Lebegue, S.; Angyan, J. G., Spin crossover transition of $Fe(phen)_2(NCS)_2$: periodic dispersion-corrected density-functional study. *PhysChemChemPhys* **2012,** *14*, 5389-5396.
46. Tarafder, K.; Kanungo, S.; Oppeneer, P. M.; Saha-Dasgupta, T., Pressure and Temperature Control of Spin-Switchable Metal-Organic Coordination Polymers from Ab Initio Calculations. *Phys. Rev. Lett.* **2012,** *109*, 077203.
47. Shao, Y.; Gan, Z.; Epifanovsky, E.; Gilbert, A. T. B.; Wormit, M.; Kussmann, J.; Lange, A. W.; Behn, A.; Deng, J.; Feng, X.; Ghosh, D.; Goldey, M.; Horn, P. R.; Jacobson, L. D.; Kaliman, I.; Khaliullin, R. Z.; Kus, T.; Landau, A.; Liu, J.; Proynov, E. I.; Rhee, Y. M.; Richard, R. M.; Rohrdanz, M. A.; Steele, R. P.; Sundstrom, E. J.; Woodcock, H. L., III; Zimmerman, P. M.; Zuev, D.; Albrecht, B.; Alguire, E.; Austin, B.; Beran, G. J. O.; Bernard, Y. A.; Berquist, E.; Brandhorst, K.; Bravaya, K. B.; Brown, S. T.; Casanova, D.; Chang, C.-M.; Chen, Y.; Chien, S. H.; Closser, K. D.; Crittenden, D. L.; Diedenhofen, M.; DiStasio, R. A., Jr.; Do, H.; Dutoi, A. D.; Edgar, R. G.; Fatehi, S.; Fusti-Molnar, L.; Ghysels, A.; Golubeva-Zadorozhnaya, A.; Gomes, J.; Hanson-Heine, M. W. D.; Harbach, P. H. P.; Hauser, A. W.; Hohenstein, E. G.; Holden, Z. C.; Jagau, T.-C.; Ji, H.; Kaduk, B.; Khistyaev, K.; Kim, J.; Kim, J.; King, R. A.; Klunzinger, P.; Kosenkov, D.; Kowalczyk, T.; Krauter, C. M.; Lao, K. U.; Laurent, A. D.; Lawler, K. V.; Levchenko, S. V.; Lin, C. Y.; Liu, F.; Livshits, E.; Lochan, R. C.; Luenser, A.; Manohar, P.; Manzer, S. F.; Mao, S.-P.; Mardirossian, N.; Marenich, A. V.; Maurer, S. A.; Mayhall, N. J.; Neuscamman, E.; Oana, C. M.; Olivares-Amaya, R.; O'Neill, D. P.; Parkhill, J. A.; Perrine, T. M.; Peverati, R.; Prociuk, A.; Rehn, D. R.; Rosta, E.; Russ, N. J.; Sharada, S. M.; Sharma, S.; Small, D. W.; Sodt, A.; Stein, T.; Stueck, D.; Su, Y.-C.; Thom, A. J. W.; Tsuchimochi, T.; Vanovschi, V.; Vogt, L.; Vydrov, O.; Wang, T.; Watson, M. A.; Wenzel, J.; White, A.; Williams, C. F.; Yang, J.; Yeganeh, S.; Yost, S. R.; You, Z.-Q.; Zhang, I. Y.; Zhang, X.; Zhao, Y.; Brooks, B. R.; Chan, G. K. L.; Chipman, D. M.; Cramer, C. J.; Goddard, W. A., III; Gordon, M. S.; Hehre, W. J.; Klamt, A.; Schaefer, H. F., III; Schmidt, M. W.; Sherrill, C. D.; Truhlar, D. G.; Warshel, A.; Xu, X.; Aspuru-Guzik, A.; Baer, R.; Bell, A. T.; Besley, N. A.; Chai, J.-D.; Dreuw, A.; Dunietz, B. D.; Furlani, T. R.; Gwaltney, S. R.; Hsu, C.-P.; Jung, Y.; Kong, J.; Lambrecht, D. S.; Liang, W.; Ochsenfeld, C.; Rassolov, V. A.; Slipchenko, L. V.; Subotnik, J. E.; Van Voorhis, T.; Herbert, J. M.; Krylov, A. I.; Gill, P. M. W.; Head-Gordon, M., Advances in molecular quantum chemistry contained in the Q-Chem 4 program package. *Mol. Phys.* **2015,** *113*, 184-215.
48. Schafer, A.; Huber, C.; Ahlrichs, R., Fully-optimized contracted gaussian-basis sets of triple zeta valence quality for atoms Li to Kr. *J. Chem. Phys.* **1994,** *100*, 5829-5835.
49. Staroverov, V. N.; Scuseria, G. E.; Tao, J. M.; Perdew, J. P., Comparative assessment of a new nonempirical density functional: Molecules and hydrogen-bonded complexes. *J. Chem. Phys.* **2003,** *119*, 12129-12137.

50. Tao, J. M.; Perdew, J. P.; Staroverov, V. N.; Scuseria, G. E., Climbing the density functional ladder: Nonempirical meta-generalized gradient approximation designed for molecules and solids. *Phys. Rev. Lett.* **2003,** *91*, 146401.
51. Sun, J.; Ruzsinszky, A.; Perdew, J. P., Strongly Constrained and Appropriately Normed Semilocal Density Functional. *Phys. Rev. Lett.* **2015,** *115*, 036402.
52. Ahlrichs, R.; Bar, M.; Haser, M.; Horn, H.; Kolmel, C., Electronic-Structure Calculations On Workstation Computers - The Program System Turbomole. *Chem. Phys. Lett.* **1989,** *162*, 165-169